

## Spin Density and Manganese Electronic Structure in Phthalocyaninato-manganese(II)

By **Brian N. Figgis** and **Geoffrey A. Williams**,\*† School of Chemistry, University of Western Australia, Nedlands, W.A. 6009, Australia

**J. Bruce Forsyth**, Neutron Division, S.R.C. Rutherford Laboratory, Chilton, Oxford OX11 0QX

**Ronald Mason**, School of Molecular Sciences, University of Sussex, Brighton BN1 9QJ

The collection of polarised neutron diffraction data for ferromagnetic ( $T_c = 8.6$  K)  $\beta$ -phthalocyaninato-manganese(II), [Mn(pc)] ( $Mn^{II}$ ,  $S = \frac{3}{2}$ ), is described. Flipping ratios for 552 unique Bragg reflections were observed at 4.2 K and at a magnetic field strength of 1.49 T applied along the  $b$  crystal axis direction. These were used, together with the 5.8 K neutron diffraction nuclear structural data, to refine by a least-squares procedure a model of the spin-density distribution in the [Mn(pc)] crystal. The magnetic moments on the two [Mn(pc)] molecules in the monoclinic cell lie approximately perpendicular to the planes of the molecules. The molecules pack in a 'herringbone' fashion, with each molecular plane inclined at *ca.*  $45^\circ$  to the monoclinic  $b$  axis. The orientation of the magnetic moments has been described in terms of two refineable angles  $\rho$  and  $\psi$ . The angle that the magnetic moment makes with the  $b$  axis,  $\rho$ , is  $37.3(7)^\circ$  and  $\psi$ , the angle the projection of the moment onto the  $ac$  plane makes with the  $a$  axis, is  $-40.3(11)^\circ$  measured in a clockwise sense towards the  $c$  axis. The model of the spin-density distribution also employed the  $3d$  and diffuse  $4s$ -type orbitals of manganese, and orbitals of the inner-ring nitrogen and carbon atoms of the macrocyclic ligand. The manganese spin populations  $3d_{xy}^{0.74(6)}$ ,  $3d_{xz, yz}^{1.17(6)}$ ,  $3d_{z^2}^{0.83(6)}$ ,  $3d_{x^2-y^2}^{-0.15(6)}$ ,  $4s^{-0.44(6)}$  were found, together with a total population of  $-0.31(3)$  spin on the macrocycle N and C atoms. The manganese orbital *electronic* populations deduced are thus  $3d_{xy}^{1.26}$ ,  $3d_{xz}^{1.0}$ ,  $3d_{yz}^{1.0}$ ,  $3d_{z^2}^{0.83}$ ,  $3d_{x^2-y^2}^{0.15}$ ,  $4s^{-1.56}$ . These orbital populations are shown to be in reasonable agreement with the predictions of an angular overlap ligand-field model treatment, and with those populations determined from an X-ray diffraction analysis of [Mn(pc)] at 116 K. The observed negative ligand spin densities, which must arise through spin polarisation effects, are in concordance with the results of a polarised neutron diffraction analysis of [Co(pc)].

THE transition-metal phthalocyanine compounds have attracted attention over many years, partly because of their relationship to the porphyrin compounds and partly because they are well characterised and of high chemical robustness. For many metal atoms they provide the best examples of a square-planar ligand environment. We have in hand a program to study the chemical bonding in certain of these compounds using the techniques of X-ray diffraction for charge-density analyses and polarised neutron diffraction for spin-density determinations.<sup>1-3</sup>

The  $\beta$ -polymorph of (phthalocyaninato)manganese(II), [Mn(pc)], is of particular interest, firstly because it is an example of manganese(II) in the unusual spin state of  $S = \frac{3}{2}$ , and secondly because it is a molecular ferromagnet, with  $T_c = 8.6$  K.<sup>4,5</sup> An earlier account<sup>2</sup> of the bonding in [Mn(pc)], based upon an X-ray diffraction data set (at 116 K) of good accuracy,<sup>6</sup> gave manganese atom  $d$ -orbital populations totalling 3.8 and a  $4s$  orbital population of 2.0 electrons and indicated that the  $3d$  radial wavefunctions were not much different from those of the free  $Mn^{2+}$  ion; it also indicated<sup>2</sup> that the charge on the manganese atom was *ca.* +1. It was suggested that the fractional  $d$ -orbital populations deduced were the result of interelectronic repulsions amongst the group of manganese orbitals  $3d_{xz}$ ,  $3d_{yz}$ ,  $3d_{z^2}$ , and  $3d_{xy}$  lying quite close together, with  $3d_{x^2-y^2}$  much higher. (The co-ordinate system is chosen with  $X$  and  $Y$  almost along the Mn-N vectors, and  $Z$  perpendicular to the molecular plane.)

The spectra of transition-metal phthalocyanine com-

† *Present address:* Australian Radiation Laboratory, Lower Plenty Road, Yallambie, Victoria 3085, Australia.

pounds are not very informative about the  $d$ -orbital separations, as they are dominated by charge-transfer bands. Consequently, the studies of their physical properties have tended to concentrate on magnetic measurements. The magnetic susceptibility and anisotropy and the magnetisation behaviour of [Mn(pc)] have been studied closely.<sup>4,5,7,8</sup> The effective magnetic moment above *ca.* 100 K is somewhat greater than the spin-only value corresponding to  $S = \frac{3}{2}$  (3.88 B.M.†) and shows little anisotropy.<sup>4</sup> These features have been accounted for in terms of ligand-field parameters for square-planar stereochemistry and their relationship to those for interelectronic repulsions and spin-orbit coupling for the  $Mn^{2+}$  ion.<sup>7</sup>

Below *ca.* 100 K the effective magnetic moment rises and goes through a maximum of 7.3 B.M. at 14 K, falling sharply below that temperature ( $H = 1.5$  T).<sup>4</sup> This behaviour was ascribed to an Ising one-dimensional linear-chain model for the magnetic exchange, with  $J = 7.6$  cm<sup>-1</sup>, together with a considerable zero-field splitting of the quartet ground term ( $D$  *ca.* 20 cm<sup>-1</sup>) and a small antiferromagnetic interchain coupling.<sup>7</sup> The compound becomes magnetically ordered below 8.6 K and exhibits a ferromagnetic moment of  $2.2 \pm 0.2$  B.M. per Mn atom parallel to the  $b$  axis in zero field. The low value of the observed saturation magnetisation compared to the expected value of 3 B.M./Mn can be understood in terms of a model in which the moments on the two [Mn(pc)] molecules in the monoclinic cell lie perpendicular to the planes of the molecules. The molecules are packed in a 'herringbone' fashion in the unit cell, with the molecular plane inclined at *ca.*  $45^\circ$  to the monoclinic

† Throughout this paper: 1 B.M. =  $9.274 \times 10^{-24}$  A m<sup>2</sup>.

*b* axis,<sup>6</sup> and aza-nitrogen atoms of adjacent molecules approaching the metal atom of each molecule towards octahedral positions. This structure provides an obvious basis for the linear-chain magnetic-exchange process.<sup>4</sup> A study of the magnetisation behaviour at very low temperatures<sup>5,8</sup> has resulted in a detailed model for the magnetic ordering. It is postulated that at low magnetic fields there are four domains which reduce to one at high fields. In the high-field region the magnetic moment vector on the manganese atom is believed to be progressively moved towards the magnetic field direction as the field becomes stronger, but the alignment along any crystal axis is not complete at 1.2 T.<sup>8</sup>

In a previous publication<sup>3</sup> we have described the application of the polarised neutron diffraction (p.n.d.) technique to the determination of the spin-density distribution in [Co(pc)]. Our analysis proceeded in terms of cobalt atom *d*-orbital populations and of chemical bonding in the molecule. In this paper we report the application of the technique to [Mn(pc)]. Because of the higher magnetisation available in [Mn(pc)] ( $S = \frac{3}{2}$ ) compared with that in [Co(pc)] ( $S = \frac{1}{2}$ ), and because the ferromagnetic ordering facilitates the experiment, it is expected that the accuracy of the data gathered will be substantially greater. We deduce manganese atom *d*- and *s*-orbital populations which can be compared both with the predictions of the ligand-field model, which accounts for the higher temperature magnetic susceptibilities, and with the populations found from the X-ray diffraction study.<sup>2</sup> We also find spin density on the ligand macrocycle, and compare it with the similar feature observed in [Co(pc)].<sup>3</sup> Our measurements have also enabled us to confirm the basic model for the ordered magnetic structure previously deduced from the magnetisation data,<sup>8</sup> and precise moment directions have been refined from our p.n.d. data.

#### EXPERIMENTAL

Large single crystals of the  $\beta$ -polymorphic form of [Mn(pc)] suitable for p.n.d. studies were grown by entrainer vacuum-sublimation techniques,<sup>9</sup> and made available by Dr. P. E. Fielding of the University of New England. Crystal data were taken from the 5.8 K neutron diffraction structure determination<sup>10</sup> [ $C_{32}H_{16}MnN_8$ ,  $M = 567.49$ , space group  $P2_1/c$ ,  $a = 1.460$  1(5),  $b = 0.469$  (1),  $c = 1.932$  7(5) nm,  $\beta = 121.10$  (1)°,  $Z = 2$ ]. P.n.d. 'flipping ratios'<sup>11</sup> were obtained at 4.2 K on the D3 normal-beam diffractometer located at a thermal neutron beam of the Institut Laue-Langevin high-flux reactor. The maximum flux available at the sample was *ca.*  $3 \times 10^{10}$  neutrons  $m^{-2} s^{-1}$ . Data were obtained at different times from the same crystal, of dimensions  $0.9 \times 1.2 \times 9.0$  mm. Two periods, totalling *ca.* 20 days use of the D3 diffractometer, were available for data collection. The crystal was aligned with its largest dimension (corresponding to the *b* axial direction) coincident with the  $\omega$ -2 $\theta$  diffractometer axis, and a magnetic field of  $1.49 \pm 0.05$  T was applied along this direction. This geometry allowed Bragg reflections *hkl* with  $k \leq 3$  to be measured. In general, *ca.* 30 min were spent on each measurement of a flipping ratio. For many of the Bragg reflections, measurements were repeated several times to improve counting

statistics and, where possible, the accessible symmetry equivalents were also measured. Only those reflections with moderate to large *nuclear* intensities were measured, as the weaker reflections required much greater measuring times for worthwhile statistical accuracy.

In the first experiment, flipping ratios were measured at  $\lambda$  98.6 pm, within the limits  $0 < (\sin\theta)/\lambda \leq 5.0$  nm<sup>-1</sup> and *hkl* with  $k \leq 2$ . The polarisation ratio (*P*) was 0.966(1) and the flipping efficiency (*E*) was 0.986(1). Corrections for the polarisation and flipping efficiencies were made and the flipping ratios were converted to  $\gamma$  values by use of previously detailed formulae,<sup>11</sup> where  $\gamma(hkl) = F_M(hkl)/F_N(hkl)$ , the ratio of magnetic [ $F_M(hkl)$ ] and nuclear [ $F_N(hkl)$ ] structure factors. For equivalent Bragg reflections,  $\gamma(hkl)$  values were combined, yielding 167 unique, non-equivalent observations. The agreement index  $A = \Sigma |\gamma - \gamma_{av.}| / \Sigma |\gamma_{av.}|$  was 0.047 for 42 pairs of equivalent reflections, where  $\gamma_{av.}$  is the relevant mean ratio of a unique observation. The standard deviation in each  $\gamma$  value,  $\sigma(\gamma)$ , was determined from counting statistics. Phased  $F_M$  values on an absolute scale (B.M./unit cell), together with standard deviations  $\sigma(F_M)$ , were obtained from the  $\gamma$  and  $\sigma(\gamma)$  values by use of  $F_N$  values calculated for a hypothetical extinction-free crystal from the 5.8 K nuclear structure refinement of [Mn(pc)].<sup>10</sup> The  $\sigma(F_M)$  values include an estimate (0.2 B.M./unit cell) of the least-squares error in  $F_N$  which arises from errors in the structural model used to calculate  $F_N$ .

In the second experiment, flipping ratios were again measured at  $\lambda$  98.6 pm, within the limits  $0 < (\sin\theta)/\lambda \leq 7.0$  nm<sup>-1</sup> and  $k \leq 2$  [ $P = 0.963$  8(5),  $E = 0.988$  2(5)]. These were converted to  $\gamma$  values as before. For equivalent Bragg reflections,  $\gamma(hkl)$  values were combined, yielding 336 unique, non-equivalent observations. The agreement index *A* was 0.096 for 68 pairs of equivalent reflections. Values of  $F_M$  and  $\sigma(F_M)$  were obtained as above. Five reflections were common to both data sets, and these were used to obtain, by a least-squares method, a scale factor of 1.027 to place the  $F_M$  data from the second experiment on the same scale as the first set of data. This small departure of the scale factor from unity probably reflects a slightly different average magnetic field on the sample in the two experiments. The agreement index  $A_F = \{ \Sigma [(F_M - F_{av.})^2 / \sigma^2(F_M)] / \Sigma [F_M^2 / \sigma^2(F_M)] \}^{1/2}$  was 0.028 for the five pairs of identical reflections, where the summations are over all 10 individual observations of  $F_M$ , and  $F_{av.}$  is the relevant mean magnetic structure factor.

In order to both check the significance of extinction effects, and to collect some data with  $k = 3$ , a number of flipping ratios were measured at  $\lambda$  79.97 pm [ $P = 0.921$  4(9),  $E = 1.000$  6(9)], and identical reflections were averaged to give 69 unique observations. Because of the significantly lower neutron flux at this wavelength, these data were not as precise as those at  $\lambda$  98.6 pm. These  $\lambda$  79.97 pm data included 54 reflections with  $k = 3$ . Both data sets were merged, with the 15 observations common to both used to obtain, by a least-squares method, a scale factor of 0.990 to place the  $\lambda$  79.97 pm data on the same scale as the  $\lambda$  98.6 pm data. The agreement index  $A_F$  was 0.017 for the 15 pairs of identical reflections. This excellent agreement between the two data sets indicates that extinction effects are insignificant, in concordance with the results of the 5.8 K nuclear structure refinement of [Mn(pc)].<sup>10</sup>

During the 5.8 K nuclear structure analysis of [Mn(pc)], the systematically absent reflections *h0l* with *l* odd in space group  $P2_1/c$  were observed to have small intensities.<sup>10</sup> The

most likely source of such intensity was shown to be multiple scattering effects rather than a change in space group at 5.8 K.<sup>10</sup> In the present analysis, it was observed that the intensities of several of the 'systematically absent'  $h0l$  reflections at low  $(\sin\theta)/\lambda$  values increased by a factor of *ca.* 2 on applying the 1.5 T magnetic field to the crystal. This effect is a direct demonstration that some part of the magnetic moment on the two Mn atoms at (000) and  $(0\frac{1}{2}0)$  in the unit cell is coupled antiferromagnetically, and can therefore give rise to magnetic scattering in reflections with  $(k+l)$  odd.

The combined set of 552 unique, non-equivalent  $F_M(hkl)$  values (including 54 with  $k=3$ ) was used in the subsequent modelling procedure described below.

**Modelling the Data.**—The least-squares refinement program ASRED<sup>12</sup> was used to optimise the parameters in a chemically based modelling of the data. This procedure, in which spin populations of *s*, *p*, or *d* orbitals on each atom are refined by a least-squares method, has been described in detail elsewhere.<sup>2,3,13,14</sup>

For the essentially planar [Mn(pc)] molecule, the *z* quantisation direction is chosen perpendicular to the  $MnN_4$  co-ordination plane for all atoms. For the Mn atom, the *x* and *y* axes were chosen along the Mn–N(2) and Mn–N(4) bonds respectively (Figure 1). The atom numbering and molecular geometry are shown in Figure 2. The model for the spin-density distribution in [Mn(pc)] was restricted to a consideration of  $3d$  orbitals, together with a spherically symmetrical diffuse  $4s$ -like orbital on  $Mn^{2+}$ , and to  $2s$  or  $2p_z$  orbital populations on the macrocyclic ligand atoms N(1), N(2), N(3), N(4), C(1), C(2), C(7), C(8), C(9), C(10), C(15), and C(16). In most refinements, based on the essential (although not crystallographic)  $D_{4h}$  symmetry of the [Mn(pc)] molecule, the populations of the  $3d_{xz}$  and  $3d_{yz}$  orbitals were constrained to be equal.

Tabulated single-electron scattering-factor curves for the  $3d$  electrons of  $Mn^{2+}$  and for the  $2p$  electrons of C and N were used.<sup>15</sup> The ' $4s$ ' scattering curve for  $Mn^{2+}$  was calculated from a wavefunction with  $\zeta = 1.8$ ,<sup>16</sup> using a published method.<sup>17</sup> Because such single-electron scattering curves apply to the theoretical free atom or ion, for real atoms in a chemical environment it is desirable to allow some expansion or contraction of the curve. This is accomplished in ASRED by a least-squares refinement of a radial parameter  $r$ , defined by  $f(s) = f_0(rs)$  where  $f(s)$  is the single-electron scattering factor at  $(\sin\theta)/\lambda = s$  and  $f_0(rs)$  is the free atom or ion scattering factor at  $(\sin\theta)/\lambda = rs$ . The refinement of  $r$

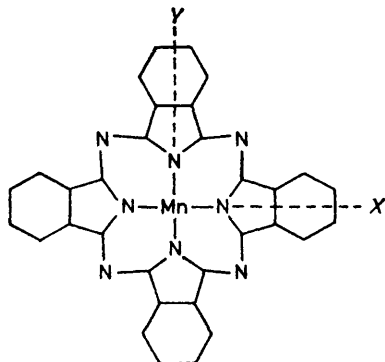


FIGURE 1 Schematic representation of the approximately planar [Mn(pc)] molecule. The *X* and *Y* axes of the co-ordinate system used throughout this discussion are indicated, and the *Z* direction is perpendicular to the  $MnN_4$  plane. Unlabelled atoms are carbon

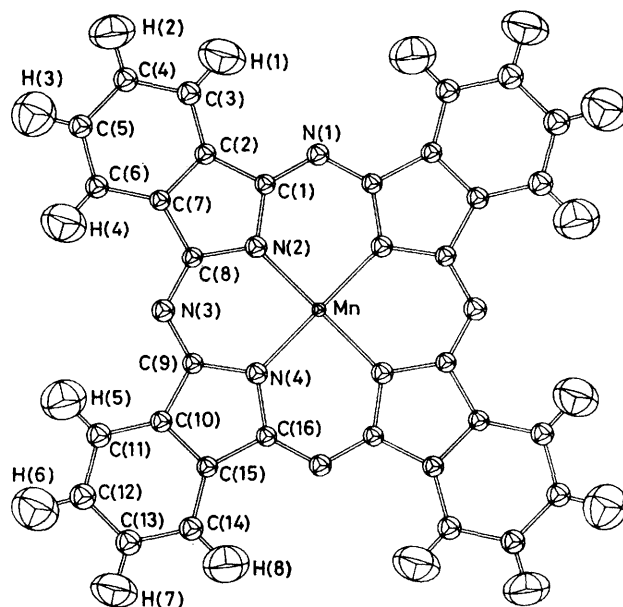


FIGURE 2 ORTEP drawing of [Mn(pc)] (5.8 K parameters, ref. 10) showing the molecular geometry and atom numbering. The thermal ellipsoids are drawn at the 99% probability level

is associated with variation of the radial exponents of the atomic wavefunction.

A correction is made for the orbital component of the magnetisation which contributes to the  $F_M$  values and which does not arise from the spin density. This orbital contribution arises from the mixing of orbitally degenerate higher states into the orbitally non-degenerate  $^4A_{2g}$  ground term by spin-orbit coupling. The dipole approximation<sup>18</sup> is used in ASRED to correct for the spherical component of the orbital contribution to  $F_M$ , in terms of the experimental gyromagnetic ratio  $g_b$  value of 2.10 (deduced from ref. 4) and the theoretical form factor  $\langle j_z \rangle_{3d}$  for a free  $Mn^{2+}$  ion.<sup>15</sup> This treatment assumes that the aspherical component of the orbital contribution is small enough that it can be neglected. In [Mn(pc)], where there is no large anisotropy in the  $g$  values, which are close to 2.0, such an assumption is undoubtedly a very good one.

An independent measurement of the magnetisation of [Mn(pc)], at 4.2 K and 1.49 T and with the magnetic field aligned along the *b* crystal axis, is not available. Therefore we have no experimental value of  $F(000)$  to use to scale the structure factor calculation from the model. Hence the spin populations from the refinements are on a relative rather than absolute scale. They are presented below on an absolute scale by assuming that all of the spin density on the molecule has been accounted for in the model, and normalizing the summation of all spin in the model to the known value of three spins per [Mn(pc)] molecule.

Our approach in modelling the aligned paramagnetism in the case of [Co(pc)] was to determine the atomic orbital occupations by a refinement process in which we modelled the 'observed' magnetic structure factors.<sup>3</sup> These  $F_M$  values were derived from the observed flipping ratios in the conventional manner, which assumes that the magnetisation vector of each molecule is coincident with the magnetic field direction, and hence with the neutron polarisation direction ( $\vec{P}$ ) in the  $D_3$  diffractometer. This is clearly not the case in the [Mn(pc)] crystal if the proposed model<sup>8</sup> for

the magnetisation at 4.2 K and high magnetic field strengths is correct. In this model, the magnetic moment vectors on each of the two molecules in the unit cell of [Mn(pc)] remain directed approximately along the normals to the molecular planes, which are at 47° to the *b* axis,<sup>10</sup> in spite of the orienting effect of the magnetic field.

An examination of the  $F_M'$  values for [Mn(pc)], which are those derived on the assumption that the magnetic moment ( $\vec{\mu}$ ) is aligned along the magnetic field direction, revealed anomalies in the  $k + l = 2n + 1$  data. In the space group  $P2_1/c$ , spherically symmetrical spin density on the Mn atom does not contribute to the class of reflections  $hkl$  with  $k + l = 2n + 1$ . Hence the  $F_M$  values of these data are expected to be small, arising only from the aspherical components of the spin density on the manganese atom and from spin density delocalised onto the macrocyclic ligand. However, the  $F_M'$  values for many of these reflections were very large. For instance, the (112) reflection had an  $F_M'$  value of 7.4(1) B.M./unit cell, whereas the largest  $k + l = 2n$   $F_M'$  value was 4.8(1) B.M./unit cell. There is no way in which the spin density on the two [Mn(pc)] molecules in the unit cell, each with  $S = \frac{3}{2}$  and  $\vec{\mu}$  aligned along the *b* axis, can be arranged to give such  $k + l = 2n + 1$   $F_M'$  values. However, by omitting the  $k + l = 2n + 1$  data entirely a satisfactory refinement of a model, similar to that employed in the case of [Co(pc)],<sup>3</sup> was obtained with the  $k + l = 2n$   $F_M'$  data.

The calculation of  $F_M$  when the magnetic moment on each scattering centre in the unit cell is not aligned along the magnetic field is somewhat involved. We have found it convenient to proceed so that the modelling of the magnetisation density in [Mn(pc)] is not directly in terms of the magnetic structure factors. Rather, it is more suitable to return to the basic experimental data, the flipping ratios [ $R(hkl)$ ]. Then (using equation 10.94 of ref. 18) we obtain equation (1) for this centrosymmetric crystal, where  $Q_i$  is

$$R(hkl) = \frac{\sum_{i=1}^2 (F_N^2 + 2F_M F_N Q_i \vec{P} + Q_i^2 F_M^2)}{\sum_{i=1}^2 (F_N^2 - 2F_M F_N Q_i \vec{P} + Q_i^2 F_M^2)} \quad (1)$$

an orientation factor which differs for the two molecules in the unit cell and is defined by  $Q_i = \vec{x} \times (\vec{\eta}_i \times \vec{x})$ , where  $\vec{P}$ ,  $\vec{x}$ , and  $\vec{\eta}_i$  are unit vectors in the directions of the polarisation of the neutrons (and of the magnetic field), the scattering vector, and the magnetic moment on the molecule respectively. Of these vectors,  $\vec{P}$  is fixed by the design of the D3 diffractometer, and  $\vec{x}$  is defined by the crystal and counter orientations.

In our modelling of the magnetisation density in [Mn(pc)], the crystallographic  $2_1$  axis is retained so that the magnetic moment directions on the molecules in the unit cell are related by a rotation of  $\pi$  about the *b* axis. The program ASRED was modified to calculate flipping ratios using equation (1). The orientation factor  $Q_i$  was calculated as a function of two angles specifying the orientation of the magnetic moment in one molecule with respect to the *b* axis.  $\rho$  is the angle that  $\vec{\eta}_i$ , say, makes with the *b* axis and  $\psi$  is the angle its projection onto the *ac* plane makes with the *a* axis, measured in a clockwise sense towards the *c* axis when viewed down *b*. The angles  $\rho$  and  $\psi$  were refined in the least-squares process.

The  $F_M'(hkl)$  data, obtained from the experimental  $R(hkl)$  values, had been corrected for incomplete beam

polarisation and flipping efficiency. Rather than develop programs to correct the experimental flipping ratios, we used the  $\gamma(hkl) = F_M'/F_N$  values and converted them to corrected flipping ratios by reversing the calculation involved in the data reduction step. Thus our corrected observed data were as in equation (2), where  $\sin^2 \alpha_{hkl} = 1 - (\vec{x} \cdot \vec{P})^2$

$$R(hkl)_o = \frac{1 + 2(\sin^2 \alpha_{hkl})\gamma(hkl) + (\sin^2 \alpha_{hkl})\gamma^2(hkl)}{1 - 2(\sin^2 \alpha_{hkl})\gamma(hkl) + (\sin^2 \alpha_{hkl})\gamma^2(hkl)} \quad (2)$$

and  $R(hkl)_o$  is the idealized flipping ratio for polarisation and flipping efficiency both unity. In order to increase the sensitivity of the agreement indices to changes in the parameters of the model, the quantity used in the refinements in ASRED was  $(1 - R_o)$ . The function minimised in the least-squares procedure was  $\sum w(\Delta R)^2$ , where  $w = 1/\sigma^2(R_o)$  is the weight assigned to the  $R_o$  values,  $\Delta R = (R_o - 1) - (R_c - 1)$ , and  $R_c$  is the calculated flipping ratio.

Our modelling of the data proceeded without giving consideration to certain possible systematic errors. In this connection it should be noted that recently we have observed an unexplained reduction in some of the magnetic structure factors at low values of  $(\sin\theta)/\lambda$  in a study of the compound  $\text{Cs}_3\text{CoCl}_5$ .<sup>19</sup> The phenomenon may be connected with multiple-scattering effects. Our data give no obvious ways of establishing whether a similar effect is likely to be present in [Mn(pc)], but if it is present, and it is large, then our deductions about the spin density delocalised onto the macrocyclic ligand are subject to some doubt.

## RESULTS

Variations of the model described above were refined using all 552 unique data. The results of the refinements are presented in Table 1. All refinements were taken to convergence. The agreement indices are defined by  $R = \sum |\Delta R| / \sum |R_o - 1|$ ,  $R' = [\sum w(\Delta R)^2 / \sum w(R_o - 1)^2]^{1/2}$ , and  $\chi^2 = \sum w(\Delta R)^2 / (n - v)$  where  $n$  and  $v$  are numbers of observations and variables respectively. The quality of the data may be judged from the index  $\sum \sigma(R_o) / \sum |R_o - 1|$ , which is 0.0792.

The simplest model attempted (Model 1, Table 1) ignores any spin density on the ligand atoms. Because the net spin on the ligand is not included in this model, the manganese *3d* and *4s* orbital populations from this refinement are on a relative scale only. The  $\chi^2$  values indicate that the model is significantly improved by the consideration of spin density in  $2p_z$  orbitals centred on each of the inner-ring ligand atoms (Model 2, Table 1).

In the case of [Co(pc)], with only one unpaired electron per molecule, the p.n.d. data were not considered to be of sufficient accuracy to include more than the inner-ring ligand atoms in the spin-density model.<sup>3</sup> However, the [Mn(pc)] data are substantially more accurate and it was considered worthwhile to include the ligand atoms C(2), C(7), C(10), and C(15) in the model. The equivalent 'pyrrole' carbon atoms in the cobalt(II) porphyrins are thought to have small but significant spin populations from an analysis of the  $^1\text{H}$  n.m.r. contact shift data.<sup>20</sup> We found that each of the spin populations on these four atoms was not significantly different from zero.

In order to keep the number of variable parameters to a minimum, and to improve the estimated standard deviations of the parameters, we have constrained some of the ligand populations to be equal by arguments of approximate symmetry, supported by similar values obtained on separate refinement. The results of this refinement are presented as

TABLE 1

Orbital spin populations and agreement factors for spin-density distribution models of the [Mn(pc)] molecule, based on 552 ( $H = 1.49$  T) data <sup>a</sup>

Atom <sup>b</sup>	Variable <sup>c</sup>	Model 1	Model 2	Model 3	Model 4 <sup>f</sup>	
Mn	$3d_{xy}$	0.70(6)	0.74(6)	0.74(6)	0.70(6)	
	$3d_{xz}, 3d_{yz}$	1.15(6)	1.17(6)	1.17(6)	1.17(6)	
	$3d_z$	0.78(6)	0.83(6)	0.83(6)	0.83(6)	
	$3d_{x^2-y^2}$	-0.14(6)	-0.15(6)	-0.15(6)	-0.13(6)	
	'4s'	-0.65(5)	-0.44(6)	-0.44(6)	-0.40(6)	
	$r(3d)$	1.105(9)	1.076(9)	1.076(9)	1.074(9)	
	$\rho$	37.7(7)°	37.3(7)°	37.3(7)°	37.1(7)°	
	$\psi$	-40.5(11)°	-40.2(11)°	-40.3(11)°	-40.3(11)°	
	N(1)	$2p_z$	0	-0.017(8)	-0.007(5)	-0.008(6)
	N(2)	$2p_z$	0	-0.050(9)	-0.046(6)	-0.059(7)
N(3)	$2p_z$	0	0.000(7)	-0.007	-0.008	
N(4)	$2p_z$	0	-0.042(9)	-0.046	-0.059	
C(1)	$2p_z$	0	-0.014(9)	-0.014(4)	-0.010(5)	
C(2)	$2p_z$	0	0	-0.004(6)	-0.007(7)	
C(7)	$2p_z$	0	0	0.007(6)	0.011(7)	
C(8)	$2p_z$	0	-0.012(9)	-0.014	-0.010	
C(9)	$2p_z$	0	-0.018(9)	-0.014	-0.010	
C(10)	$2p_z$	0	0	-0.004	-0.007	
C(15)	$2p_z$	0	0	0.007	0.011	
C(16)	$2p_z$	0	-0.004(10)	-0.014	-0.010	
$R$		0.103	0.101	0.102	0.103	
$R'$		0.057	0.052	0.052	0.052	
$\chi^2$		4.995	4.272	4.260	4.234	
No. of Variables		8	16	13	13	

<sup>a</sup> A parameter which has been varied in the least-squares refinement is given an estimated standard deviation in brackets. Other parameters were either fixed at zero, or constrained to equal another variable, having the final value quoted. <sup>b</sup> The Mn, N, and C centres are at the positions and have the thermal parameters determined from the 5.8 K neutron diffraction structural analysis.<sup>10</sup>

<sup>c</sup> The symbols  $s$ ,  $p$ , and  $d$  are used here to represent populations of the corresponding orbitals. A negative spin population indicates spin density antiparallel to that of positive sign. Where two symbols appear on the one line, the population quoted refers to each orbital individually. The radial expansion parameter for the  $3d$  orbitals,  $r(3d)$ , is defined in the text. For all other orbitals,  $r$  was fixed at unity. All orbital populations have been normalized to give three unpaired electrons per [Mn(pc)] molecule; in this process, spin density on the centrosymmetrically related ligand atoms has also been taken into account. The angles  $\rho$  and  $\psi$  are defined in the text. <sup>d</sup> For Model 4 only, the ligand atom populations are for spherical  $2s$  rather than  $2p_z$  orbitals.

Model 3, Table 1. This refinement was also repeated using spherically symmetric  $2s$  orbitals, rather than  $2p_z$  orbitals, centred on each of the ligand N and C atoms. The results (Model 4, Table 1) are essentially unchanged, with the ligand  $s$ -orbital model slightly preferred on the basis of the  $\chi^2$  values. However, the data do not define well the angular variation of the spin densities on the ligand atoms.

The refinement of Model 3 was also repeated with the constraint that the manganese  $3d_{xz}$  and  $3d_{yz}$  populations be equal, removed. This refinement (14 variables) converged with  $3d_{xz}$  1.19(7),  $3d_{yz}$  1.15(7), and  $\chi^2$  4.267. All other parameters refined to identical values to those found in the Model 3 refinement. This result indicates that the assumption of essential  $D_{4h}$  symmetry for the [Mn(pc)] molecule is valid.

In order to obtain a value of  $F(000)$  from the refined values of Model 3, those values were used in a refinement based on magnetic structure factors, as was done in the [Co(pc)] p.n.d. analysis.<sup>3</sup> Only the 380  $hkl$  reflections with  $h + l = 2n$  were used, and all orbital populations for the Mn and ligand atoms were constrained at the values found in Model 3, with only the scale factor being varied. By extrapolation of the molecular magnetic form factor to  $(\sin\theta)/\lambda = 0.0$ , a value for  $F(000)$  of 4.30 B.M./unit cell was obtained. Although we cannot give a proper estimate of the error in this value, it is quite accurately determined by the experiment. This is because the low  $(\sin\theta)/\lambda$  data are the most accurate, and extend to relatively low  $(\sin\theta)/\lambda$  values because of the large unit cell, and because the ligand forward peak in the form factor is included in the scattering model. This value of  $F(000)$  corresponds to the magnetic moment,  $\langle \mu_b \rangle$ , at a magnetic field strength of 1.49 T.

Observed and calculated flipping ratios (Model 3, Table 1) are listed in Supplementary Publication No. SUP 23076 (8 pp.).\* Data reduction and statistical analyses were performed using the University of Western Australia computer programs.<sup>12</sup> All computations were performed on a CDC CYBER 73 computer at the Western Australian Regional Computing Centre.

#### DISCUSSION

*Manganese Orbital Populations.*—The most obvious features of the manganese atom  $d$ -orbital spin populations which we have deduced, as set out in Table 1, are first that they are essentially independent of the model, and secondly that the  $e_g$  ( $d_{xz}, d_{yz}$ ) values are physically unreal. The lack of dependence on model is a reflection of the fact that the models differ only in the role they allow the ligand spin distribution to play, and that this distribution is always much more diffuse in character than that of the metal  $d$  orbitals. When no ligand spin is permitted (Model 1), the diffuse information contained in the data is modelled in the next best way; the spin which in other models is on the ligand, is placed in the most diffuse area available, which is the manganese '4s' orbital.

Our analysis places 1.17 spin units in each of the members of the  $e_g$  orbital, a result which is, of course,

\* For details see Notices to Authors No. 7, *J. Chem. Soc., Dalton Trans.*, 1980, Index issue.

physically unreal. It would have been possible for us to constrain these populations to a maximum of 1.00, but we decided that it was preferable not to introduce possible bias into our analyses by using that procedure. We prefer to regard the 'excess' of 0.17 spins over unity as an estimate of the accuracy of our determination of spin populations. In our analysis of the more accurate data on  $\text{Cs}_3\text{CoCl}_5$ <sup>14</sup> we concluded that an uncertainty of 0.1 spins was inherent in each individual  $d$ -orbital population deduced. It is not surprising that an error of as large as 0.17 spin units arises in the present case. We note that the goodness-of-fit of even our best model (Model 4) is higher than we have obtained with other p.n.d. data.<sup>3,13,14</sup> There may well be some features of the magnetic ordering in  $[\text{Mn}(\text{pc})]$ , or of the participation of other manganese orbitals, which we have failed to model, and that failure could influence the  $d$ -orbital populations we report. However, in the following discussion we shall enforce physical reality and assign the total  $e_g$  orbital population as 2.00, as to do otherwise creates confusion.

In order to proceed from our spin populations to electron populations it is necessary to have guidance from other sources about the manganese atom electronic structure. We require to know whether it is likely that the spin in an orbital arises from a less-than-half-filled or from a more-than-half-filled situation (except for the  $e_g$  orbitals which now are taken to be half-filled). The magnetic susceptibility behaviour in the 100 to 300 K temperature range makes it clear that the ground term of  $[\text{Mn}(\text{pc})]$  is a spin quartet<sup>4,7</sup> with very little orbital contribution to the magnetic moment (and consequently to the  $g$  values), and a zero-field splitting corresponding to  $D$  ca. 40  $\text{cm}^{-1}$ . The  ${}^4A_{2g}$  term of  $D_{4h}$  symmetry is strongly indicated. The ground terms arising from the  $d^5$  configuration as the stereochemistry is changed from octahedral to square-planar, and with varying interelectronic repulsion parameters, have been examined employing a very flexible crystal-field model and cubic-field wavefunctions.<sup>21</sup> Both positive and negative values for  $D$  were found to arise. The results were used to analyse the magnetic susceptibility data for  $[\text{Mn}(\text{pc})]$ .<sup>7</sup> It would be possible to project out the individual  $d$ -orbital populations contained in the eigenvector suggested for the ground term of  $[\text{Mn}(\text{pc})]$ , but we have preferred a more direct and restrictive approach. We use the angular overlap model (a.o.m.)<sup>22,23</sup> for ligand-field effects, and solve the matrices of order 64 and 62 which arise from the simultaneous perturbation of the entire  $d^5$  manifold, in the  $(l, m_l; s, m_s)$  quantisation scheme. The Hamiltonian is as in equation (3), where the first

$$H = \sum e^2/r_{ij} + V_{\text{LF}} + \sum \zeta_{3d} l_i \cdot s_i \quad (3)$$

term represents the interelectronic repulsion, the second the ligand field, and the third the spin-orbit coupling effects. The interelectronic repulsions were specified in terms of the Condon-Shortley parameters  $F_2$  and  $F_4$ ,<sup>24</sup> the ligand field term by the a.o.m. parameters, and  $\zeta_{3d}$  is the single electron spin-orbit coupling parameter.

The solutions to this treatment of the problem are directly available as single-electron  $d$ -orbital populations.

We employed values of  $F_2$  and  $F_4$  for the free  $\text{Mn}^{2+}$  ion (1 440 and 96  $\text{cm}^{-1}$  respectively), and also values somewhat reduced from that situation, and a.o.m. parameters  $e_\sigma$  and  $e_\pi$  for the nitrogen ligands.  $e_\sigma$  was set at 12 000  $\text{cm}^{-1}$ , the figure we employed previously in connection with  $[\text{Co}(\text{pc})]$ .<sup>3</sup> It has been pointed out that the relative scaling of the interelectronic repulsion and the ligand-field parameters cannot be determined from the magnetic susceptibility data alone.<sup>21</sup> For the metal phthalocyanines, the  $d$ - $d$  absorption spectra are not available to help determine this scaling. We set  $\zeta_{3d} = 250$   $\text{cm}^{-1}$ , somewhat below the free-ion value, and allowed the ratio  $F = e_\pi/e_\sigma$  to vary in order to change the relationship between the low-lying terms of the  $d^5$  configuration. The results are summarised in Figure 3.

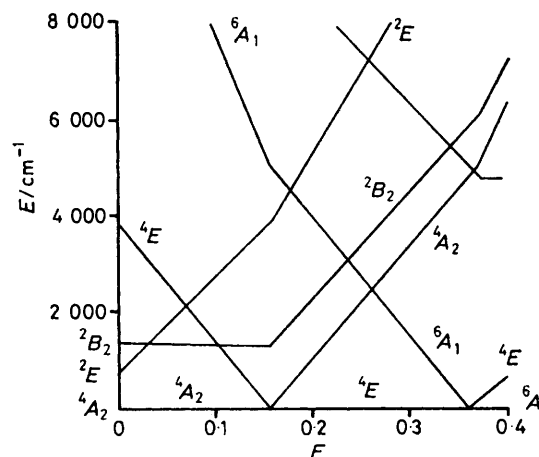


FIGURE 3 The relationship between the lower-lying terms of the  $d^5$  configuration for square-planar co-ordination, using an angular overlap model with  $e_\sigma = 12\,000$   $\text{cm}^{-1}$  and  $F = e_\pi/e_\sigma$ , and interelectronic repulsion parameters  $F_2 = 1\,100$  and  $F_4 = 80$   $\text{cm}^{-1}$

The ground term is  ${}^4A_{2g}$  for a range of small values of  $F$ , changing to  ${}^4E_g$  or  ${}^6A_{1g}$  at  $F$  ca. 0.2, depending on the relationship between the interelectronic repulsion and the a.o.m. parameters. The  ${}^4A_{2g}$  term suffers zero-field splitting from close-lying higher terms although, as pointed out previously, the influence of the  ${}^4E_g$  term is small. In the region where the  ${}^4A_{2g}$  ground term is well separated from higher terms the composition is very closely  $b_{1g}^2, e_g^2, a_{1g}^1 [d_{xy}^2, (d_{xz}^1, d_{yz}^1), d_{z^2}^1]$  and the zero-field splitting is small. When, for example, the  ${}^6A_{1g}$  term lies close above, the zero-field splitting rises and the purity of the occupational numbers falls. For instance, for a  ${}^4A_{2g}$ - ${}^6A_{1g}$  separation of 500  $\text{cm}^{-1}$ ,  $D$  is ca. 50  $\text{cm}^{-1}$ , although the  $d$ -orbital occupation numbers are still not far from integral, viz.  $d_{xy}^{1.80}, d_{xz}^{1.00}, d_{yz}^{1.00}, d_z^{0.97}, d_{x^2-y^2}^{0.21}$ . The value of  $\bar{g}$  in this region is ca. 2.2, with  $g_{\parallel} = 2.0$ , in fair agreement with experimental magnetic susceptibility data.<sup>4</sup> For any reasonable set of a.o.m. parameters we found the zero-field splitting always to be positive. If the  ${}^4A_{2g}$ - ${}^6A_{1g}$  separation is allowed to become very small,  $d$ -orbital populations far from integral are pre-

dicted, but the corresponding magnetic susceptibility behaviour would be complicated and not in agreement with experiment. We also investigated the region where the ground term is  ${}^4E_g$ , including permitting departure from  $D_{4h}$  symmetry so as to lift the degeneracy of the  $d_{xz}$  and  $d_{yz}$  orbitals. The magnetic susceptibility data are not reproduced well and, of course, when the  $d_{xz}$  and  $d_{yz}$  orbitals are no longer degenerate their populations are highly unequal. It was observed, however, that a zero-field splitting parameter of either sign could be obtained, depending upon the relationship between the a.o.m. parameters.

The guidance obtained from the foregoing investigation of a ligand-field model in conjunction with the magnetic susceptibility data is that the ground term is indeed  ${}^4A_{2g}$ , that the  $b_{2g}$  orbital is more than half-full, that the  $e_g$  and  $a_{1g}$  orbitals are half-full or less, and that the  $b_{1g}$  orbital population should be small. We use these deductions to obtain  $d$ -orbital electron populations based on Model 3, as listed in Table 2.

TABLE 2

Comparison of spin and electron populations (in electrons) in [Mn(pc)], based upon Model 3, with results from the X-ray study on the compound, from the angular overlap ligand-field model (a.o.m.) treatment, and the results for [Co(pc)]

Orbital/atom	[Mn(pc)] p.n.d.	[Mn(pc)] X-ray <sup>a</sup>	[Mn(pc)] a.o.m. calculation <sup>b</sup>	[Co(pc)] p.n.d. <sup>c</sup>
$e_g$ ( $3d$ )	2.00(20)	1.3(3)	2.00	3.66(20)
$b_{2g}$	1.26(15)	1.5(2)	1.80	1.60(15)
$a_{1g}$	0.83(15)	0.9(2)	0.97	1.21(15)
$b_{1g}$	0.15(15)	0.1(2)	0.21	0.21(15)
$a_{1g}$ (' $4s$ ')	1.56(15)	2.0(3)		1.86(20)
N(2), N(4)	-0.046(6) spin			-0.012(10) spin
N(1), N(3)	-0.007(5) spin			-0.020(5) spin
C(1), C(8), C(9), C(16)	-0.014(4) spin			-0.006(8) spin
Total ligand	-0.31(3) spin			-0.17(5) spin

<sup>a</sup> From ref. 2. <sup>b</sup> Parameters:  $F_2 = 1\ 300$ ,  $F_4 = 95$ ,  $e_\sigma = 12\ 000$ ,  $e_\pi = 1\ 920$ ,  $\zeta_{3d} = 250\ \text{cm}^{-1}$ . <sup>c</sup> From ref. 3. The ligand spin populations have been averaged where necessary to conform with the sets for [Mn(pc)].

We may compare the  $d$ -orbital electron populations with the values obtained from the analysis of an X-ray diffraction experiment,<sup>2</sup> also listed in Table 2. There is certainly broad agreement between the results of the two experiments; if an e.s.d. of *ca.* 0.15 is placed upon the p.n.d. populations and with one of 0.2 upon the X-ray populations, the agreement is within experimental error, except perhaps for the  $e_g$  set, where the p.n.d. result is distinctly the higher. The results from both the X-ray experiment, and more particularly from the p.n.d. experiment, are not in particularly good agreement with the predictions of the theory based upon the a.o.m. ligand-field treatment. The populations arising from a typical set of a.o.m. parameters giving values of  $D$  and  $g$  in concordance with the experimental magnetic susceptibility data are listed in Table 2. It is seen that the ratio of the  $b_{2g}$  ( $d_{xy}$ ) population to those of the other  $d$  orbitals is lower than the theory can reproduce. A reduction of the  $d$ -orbital populations might well be expected because of  $\pi$ -covalence effects, but the  $b_{2g}$  orbital is not expected to be involved in such bonding to the ligand as much as is the  $e_g$  orbital. Also, direct spin transfer by covalent interactions would place

positive spin on the ligand macrocycle, and that is the opposite to our observation (see below). Although the occupation number for the  $b_{1g}$  ( $d_{x^2-y^2}$ ) orbital is similar in both diffraction experiment results and in the ligand-field theory analysis, the p.n.d. experiment requires the spin to be of the opposite sign to that in the other  $d$  orbitals, and the significance of this is not clear in the level of analysis that we are attempting. The total  $d$ -orbital population is found to be 4.2 electrons, quite significantly lower than the number of five electrons required for a formal  $\text{Mn}^{2+}$  ion, and probably not significantly different from the X-ray result of 3.8 electrons.<sup>2</sup>

The a.o.m. ligand-field treatment employed above predicts that in the region where  ${}^4A_{2g}$  is the ground term, the  $d$ -orbital energy sequence in [Mn(pc)] is  $e_g < b_{2g} < a_{1g} \ll b_{1g}$ , although, on account of interelectronic repulsions, the configuration in the absence of low-lying excited terms is  $e_g^2, b_{2g}^2, a_{1g}^1$ . The four lower orbitals form a fairly closely spaced group, with the  $a_{1g}$  orbital lying within *ca.* 8 000  $\text{cm}^{-1}$  of the  $e_g$  pair. This ordering

is different to, and the spacing is not as close as, that which is required to account for the magnetic properties and the p.n.d. experiment for [Co(pc)].<sup>3</sup> In that molecule the  $d$ -orbital sequence is  $a_{1g} < e_g < b_{2g} \ll b_{1g}$ , covering a range of only *ca.* 5 000  $\text{cm}^{-1}$ . (Note the labelling of the  $d$  orbitals is different in ref. 3 because the symmetry chosen there was  $C_{2v}$  rather than  $D_{4h}$ .) Since the same value of  $e_\sigma$  has been chosen for the two compounds, the different ordering is reflected in the values assigned to the ratio  $F = e_\pi/e_\sigma$ . Values of *ca.* 0.5 were used for [Co(pc)], while in the present analysis *ca.* 0.2 is required. The ordering differs from that we suggested earlier<sup>2</sup> in that the order of the  $a_{1g}$  and  $b_{2g}$  orbitals is reversed.

The occupation number for the manganese  $4s$ -like orbital was found to be -0.44 spins. Two possibilities arise: that the ' $4s$ ' electron population is 0.44, with spin aligned opposite to that of the majority of the  $d$  electrons, or that it is 1.56, with the -0.44 spins representing the resultant 'hole' in the filled ' $4s$ ' orbital. Our experiment cannot distinguish between these possibilities. However, the X-ray result<sup>2</sup> for the ' $4s$ ' population is 2.0, and the nearly filled orbital option gives better agreement and also a more reasonable total net

charge on the manganese atom,  $\text{Mn}^{1.2+}$ , as compared with  $\text{Mn}^{2.32+}$  if the nearly empty option is chosen. In our analysis, then, the charge on the manganese atom is *ca.* +1, obtained primarily by the loss of a  $3d$  electron rather than of a  $4s$  electron. Our treatment of the X-ray diffraction data on the compound yielded a similar conclusion.

The negative spin in the  $b_{1g}$  orbital and in the '4s' orbital can arise only through spin polarisation effects. Spin polarisation arises because 'up' spin, say, tends to create more 'up' spin in its own vicinity, and corresponding 'down' spin elsewhere. It is a manifestation of electron correlation and as such is very difficult to treat in a quantitative fashion in a system as large as a transition-metal ion. Since they are of the same  $a_{1g}$  symmetry, direct spin polarisation of the '4s' orbital by the  $d_{z^2}-a_{1g}$  orbital is possible, although then presumably the  $d_{z^2}$  population would have been found to be anomalously high. Perhaps more likely is the general polarisation of the core electrons by the four  $d$  orbitals containing positive spin, and consequent polarisation by the core of the remaining  $d$  orbital and of the '4s' orbital.

*Ligand Orbital Populations.*—There is evidence for negative spin on the majority of the 'inner ring' atoms of the ligand, but for little if any on the benzene rings. The amount of spin on any individual atom is, of course, relatively small,  $-0.05$  spins at most. As might be expected, the highest spin density occurs at the four nitrogen donor atoms of the ligand macrocycle. The same effect was observed in our analysis of the p.n.d. experiment on  $[\text{Co}(\text{pc})]$ .<sup>3</sup> For the carbon atoms of the 'inner ring', C(1), C(8), C(9), and C(16), the presence of spin is also quite distinct, being significant at the  $3\sigma$  level. For the aza-bridge nitrogen atoms, N(1) and N(3), the significance of the very small negative spin populations is below the  $2\sigma$  level, and that applies also to the very small positive or negative spins indicated at the carbon atoms investigated in each benzene ring system, C(2), C(7), C(10), and C(15). The information obtained about the individual atom spin populations is not sufficiently accurate to make any comparison with, say, the Hückel-type molecular orbital coefficients obtained in the treatment of the related metal porphyrins.<sup>25</sup>

Although the individual macrocycle spin populations are, except for N(2) and N(4), not defined at a high confidence level, the total spin on the ligand macrocycle is quite clearly established and is  $-0.31$  spins, with an estimated standard deviation of 0.03. Some 10% of the total spin is associated with the macrocyclic ligand. This result may be compared with  $-0.17(5)$  spins or *ca.* 15% obtained for the entirely analogous compound  $[\text{Co}(\text{pc})]$ .<sup>3</sup> Although the spin quantum number of the manganese atom in  $[\text{Mn}(\text{pc})]$ ,  $\frac{3}{2}$ , is three times that of the cobalt atom in  $[\text{Co}(\text{pc})]$ , it is not clear that the spin density on the ligand would be expected to be exactly in that ratio,<sup>25</sup> even if the mechanism for spin transfer from the metal atom is identical in the two cases. However, the larger ligand spin density in  $[\text{Mn}(\text{pc})]$  is certainly consistent with the higher total spin of the system.

Again, the ligand spin density being negative, it must arise through spin polarisation by the larger positive spin in the manganese atom  $d$  orbitals. The mechanism proposed for spin transfer in metalloporphyrin compounds in connection with contact-shift n.m.r. data involves<sup>20</sup> charge transfer from a filled ligand  $\pi$  orbital to the metal  $e_g$  ( $d_{\pi} = d_{xz}, d_{yz}$ ) orbitals. If the metal  $e_g$  orbitals are less than half full, positive spin is taken to be preferred on the metal atom, leaving negative spin on the ligand donor atoms. If they are more than half full the metal atom would have to accept negative spin, leading to positive spin on the ligand. This mechanism would suggest that spin polarisation transfer should differ between  $[\text{Mn}(\text{pc})]$ , where the  $e_g$  orbitals are half-filled, and  $[\text{Co}(\text{pc})]$ , where they are filled. In fact, the spin transfer in the two compounds seems to be quite similar in nature.

It was suggested that in  $[\text{Co}(\text{pc})]$  the transfer of negative spin to the ligand might involve the covalent interaction of the spin-polarised '4s' orbital with the  $\sigma$ -bonding framework of the ligand. Since the amount of negative spin in the '4s' orbital is about twice as large in  $[\text{Mn}(\text{pc})]$  as in  $[\text{Co}(\text{pc})]$ , the number of spins transferred to the ligand would be twice as large, and that is what we observe.

*Magnetic Properties.*—The magnetisation studies at 4.2 K on  $[\text{Mn}(\text{pc})]$  at high magnetic field strengths<sup>4,5</sup> have been interpreted<sup>8</sup> in terms of a magnetic moment on each manganese atom, which is required to be directed approximately along the normal to the plane of the molecule by the magnetic exchange. The ground quartet state of the manganese atom was deduced to undergo a large *negative* zero-field splitting ( $|D| \gg 1 \text{ cm}^{-1}$ ), so that the effective spin quantum number at very low temperatures is  $S' = \frac{1}{2}$  made up of the  $M_s = \pm \frac{3}{2}$  components of the  $S = \frac{3}{2}$  term. The higher temperature magnetic susceptibility data<sup>4,7</sup> ( $T \gg |D|/k$ ) correspond to the  $S = \frac{3}{2}$  term with  $g_b = 2.10$ . For the low temperature case, with  $S' = \frac{1}{2}$ , we have then  $g_b = 6.3$ . The value of the moment on each Mn atom is expected to be  $gS' = 3.15$  B.M. The moment was found<sup>8</sup> to lie at *ca.*  $45^\circ$  to the  $b$  axis, so that  $\langle \mu_b \rangle = M_b/N\beta$  ( $N = \text{Avagadro's number}$ ) is expected to be  $3.15 \cos 45^\circ = 2.23$  B.M., where  $M_b = \chi_b^{\text{Mn}} H$  is the molar magnetisation, and  $\chi_b^{\text{Mn}}$  is the atomic susceptibility, each directed along the  $b$  axis of the crystal. An extrapolation of the magnetisation data to zero magnetic field strength leads to a value of  $2.2 \pm 0.2$  B.M. per molecule for  $\langle \mu_b^0 \rangle$ , which compares well with the expected value. With increasing strength of the applied field along  $b$ , the magnetic moment vector on each molecule is expected to more closely align with the  $b$  axis and the observed value of  $\langle \mu_b \rangle$  is expected to increase.

The p.n.d. experiment on  $[\text{Mn}(\text{pc})]$ , with a magnetic field of 1.49 T applied along the  $b$  crystal axis, yields a value for  $F_{\text{M}}(000)_b$  which corresponds to a magnetic moment  $\langle \mu_b \rangle$  of 4.30 B.M. per cell, or 2.15 B.M. per molecule. The magnetic moment on each manganese atom is deduced to lie at  $37.3(7)^\circ$  to the  $b$  axis, and is to



be compared with the inclination of the normal to the molecular plane to that axis at 5.8 K ( $47.4^\circ$ ).<sup>10</sup> The value of the observed moment along the *b* axis is lower than the expected value,  $3.15\cos 37.3^\circ = 2.51$  B.M.

As Miyoshi's interpretation<sup>8</sup> of the magnetisation data for [Mn(pc)] does not define the orientation of the projection of the molecular magnetic-moment vector onto the *ac* plane, he assumes that it lies approximately along the normal to the molecular plane. From the 5.8 K crystal structure determination,<sup>10</sup> the projection of the normal to the molecular plane makes an angle of  $-40.1^\circ$  to the *a* axis in the *ac* plane, measured clockwise towards *c* when viewed down *b*. The p.n.d. experiment gives the corresponding angle for the projection of the molecular magnetic-moment vector as  $-40.3(11)^\circ$ , and so proves that the vector is indeed aligned nearly along the normal.

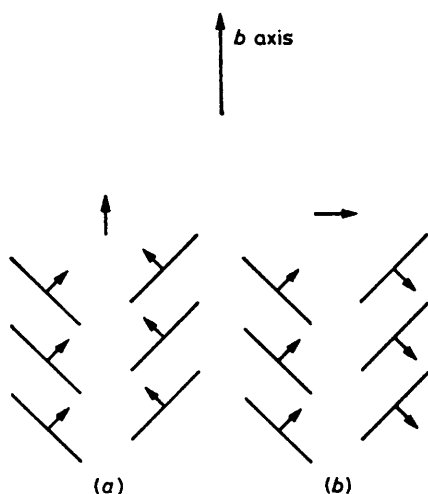


FIGURE 4 Magnetic moment orientations in the domains of [Mn(pc)] in the ferromagnetic region. Two of the four domain structures possible on the model are illustrated. The remaining two are obtained from these by inverting the individual moments through the manganese centre, and thus reversing the directions of the net moments

The model<sup>8</sup> of the low temperature magnetisation behaviour in [Mn(pc)] is based upon two ferromagnetic sublattices, each consisting of a chain of parallel magnetic moments located on the members of a row of molecules formed by the 'herringbone' stacking down the *b* crystal axis, as shown in Figure 4. The moments lie approximately along the normals to the molecular planes, and in a particular chain may be aligned in either of two directions related by an inversion centre at the manganese atom. Then, depending upon the relative orientations of the two sublattices, four domains are possible. The orientation relationships are caused by the interchain magnetic exchange, but can be affected by an external magnetic field. If the field is above *ca.* 350 mT it switches all the domains into a single one in which the maximum component of each molecular moment is aligned in the direction of the magnetic field. For the magnetic field employed in the p.n.d. experiment, 1.5 T along the *b* axis, the single domain is that of Figure 4(a).

That domain structure formed the basis for our refinement of the p.n.d. flipping ratio data.

It must be pointed out, however, that in one aspect the magnetisation model we have used is unsatisfactory. It requires that, while large, *D* be negative in sign. The higher temperature magnetic susceptibility data and our a.o.m. ligand-field analysis strongly support a positive value of this zero-field splitting parameter. If *D* is positive the mechanism of spin alignment proposed by Miyoshi<sup>8</sup> leads again to ferromagnetic ordering, provided the inter-chain magnetic-exchange coupling constant is also positive. However, then the alignment of the molecular magnetic moments is in the *ac* plane, and the ferromagnetism is not of the 'canted' type which is strongly indicated by the magnetisation behaviour and which forms the basis for our modelling of the p.n.d. data.

We thank the S.R.C. for support. G. A. W. thanks the Australian Institute of Nuclear Science and Engineering for a Research Fellowship and the University of Melbourne for a Travelling Scholarship. We are grateful to the Institut Laue-Langevin for the neutron diffraction facilities made available, and to Drs. Jane Brown and Francis Tasset in particular for their help with the D3 diffractometer.

[1/215 Received, 9th February, 1981]

#### REFERENCES

- B. N. Figgis, R. Mason, A. R. P. Smith, and G. A. Williams, *J. Am. Chem. Soc.*, 1979, **101**, 3673.
- B. N. Figgis, E. S. Kucharski, and G. A. Williams, *J. Chem. Soc., Dalton Trans.*, 1980, 1515.
- G. A. Williams, B. N. Figgis, and R. Mason, *J. Chem. Soc., Dalton Trans.*, 1981, 734.
- C. G. Barraclough, R. L. Martin, S. Mitra, and R. C. Sherwood, *J. Chem. Phys.*, 1970, **53**, 1638.
- H. Miyoshi, H. Ohya-nishiguchi, and Y. Deguchi, *Bull. Chem. Soc. Jpn.*, 1973, **46**, 2724.
- R. Mason, G. A. Williams, and P. E. Fielding, *J. Chem. Soc., Dalton Trans.*, 1979, 676.
- C. G. Barraclough, A. K. Gregson, and S. Mitra, *J. Chem. Phys.*, 1974, **60**, 962.
- H. Miyoshi, *J. Phys. Soc. Jpn.*, 1974, **37**, 50.
- P. E. Fielding and A. G. MacKay, *Aust. J. Chem.*, 1964, **17**, 750.
- B. N. Figgis, R. Mason, and G. A. Williams, *Acta Crystallogr.*, 1980, **B36**, 2963.
- P. J. Brown, J. B. Forsyth, and R. Mason, *Philos. Trans. R. Soc. London, Ser. B*, 1980, **290**, 481.
- B. N. Figgis and G. A. Williams, unpublished work.
- B. N. Figgis, P. A. Reynolds, and G. A. Williams, *J. Chem. Soc., Dalton Trans.*, 1980, 2348.
- B. N. Figgis, P. A. Reynolds, and G. A. Williams, *J. Chem. Soc., Dalton Trans.*, 1980, 2339.
- 'International Tables for X-Ray Crystallography,' Kynoch Press, Birmingham, 1974, vol. 4, pp. 103-146.
- E. Clementi and C. Roetti, *At. Data Nucl. Data Tables*, 1974, **14**, 177.
- J. Avery and K. J. Watson, *Acta Crystallogr.*, 1977, **A33**, 679.
- W. Marshall and S. W. Lovesey, 'Theory of Thermal Neutron Scattering,' Clarendon Press, Oxford, 1971.
- B. N. Figgis, P. A. Reynolds, G. A. Williams, R. Mason, A. R. P. Smith, and J. N. Varghese, *J. Chem. Soc., Dalton Trans.*, 1980, 2333.
- G. N. La Mar and F. A. Walker, *J. Am. Chem. Soc.*, 1973, **95**, 1790.
- G. Harris, *Theor. Chim. Acta*, 1968, **10**, 119.
- C. E. Schäffer, *Struct. Bonding (Berlin)*, 1968, **5**, 68.
- J. Glerup, O. Monsted, and C. E. Schäffer, *Inorg. Chem.*, 1976, **15**, 1399.
- E. U. Condon and G. H. Shortley, 'The Theory of Atomic Spectra,' Cambridge University Press, 1957.
- R. G. Shulman, S. H. Glarum, and M. Karplus, *J. Mol. Biol.* 1971, **57**, 93.